AIAA JOURNAL
Vol. 35, No. 2, February 1997

Forced Response of Coupled Substructures Using Experimentally Based Component Mode Synthesis

Jeffrey A. Morgan*
General Motors Corporation, Warren, Michigan 48090-9060
and
Christophe Pierre† and Gregory M. Hulbert‡
University of Michigan, Ann Arbor, Michigan 48109-2125

A new method is presented to calculate the forced response of coupled substructures using experimentally based component mode synthesis (CMS). The method uses test-derived CMS matrices and the uncoupled forced response of each substructure to predict the coupled-system forced response. This is achieved by considering the internal coupling forces and external applied forces on a substructure independently, and superimposing the responses of each. The advantage of this approach is that any number of applied forces can be present, and these can occur at unmeasurable locations. Periodic excitations are considered, and the analysis is performed in the frequency domain. The method is ideally suited for integrating test-derived models with finite element models for forced response predictions. A test case is conducted for a simple plate–beam system. The method is simulated analytically, then conducted experimentally using actual measured data. Good correlation is achieved for both cases.

Nomenclature

B	= system matrix
C	= damping matrix
d_0	= cone base diameter
E	= modulus of elasticity
$\boldsymbol{F}$	= force vector
I	= identity matrix
i	= imaginary number; $\sqrt{-1}$
K	= stiffness matrix
k_c	= coupling stiffness
L	= cone length to tip
M	= mass matrix
N	= total number of substructures
S	= cone length to frustrum
T	= transformation matrix
$\boldsymbol{X}$	= response vector
$\hat{\boldsymbol{X}}$	= response vector due to external forces
$\tilde{\boldsymbol{X}}$	= response vector due to coupling forces
x, y, z	= coordinate directions
α	= structural damping coefficient
Υ, Ψ	= partitioned transformation matrices
υ	= Poisson's ratio
ω	= frequency, rad/s

Subscripts

a	= active degrees of freedom (DOF)
c	= coupling DOF
cb	= Craig–Bampton type
n	= noncoupling DOF
o	= omitted DOF
s	= modal DOF

Superscript

(j)	= substructure identification number

Received March 13, 1996; revision received Oct. 23, 1996; accepted for publication Oct. 24, 1996; also published in *AIAA Journal on Disc*, Volume 2, Number 2.

*Senior Project Engineer, Engineering Analysis Department, General Motors Powertrain Division, Mail Loc. 480-723-828, 30003 Van Dyke Avenue.
†Associate Professor, Department of Mechanical Engineering and Applied Mechanics, 2204 G.G. Brown. Senior Member AIAA.
‡Associate Professor, Department of Mechanical Engineering and Applied Mechanics, 2250 G.G. Brown.

I. Introduction

An experimentally based method of component mode synthesis (CMS) has been developed,[1,2] which enables CMS matrices to be determined from test. This allows for the calculation of the natural frequencies and mode shapes for systems of coupled substructures using measured data. The present paper extends this method to include coupled forced-response predictions based on uncoupled response data. The motivation for the development of the method is the relatively poor performance of existing force estimation methods under the typical conditions of application, i.e., many forces applied at unmeasurable locations. The usual problems associated with these force estimation methods are completely bypassed using superposition of responses instead of force estimation. This allows forced response to be accurately predicted from measured data.

One common approach to forced-response predictions is to estimate the applied forces and then apply them to the coupled-system model. Two popular methods of force estimation are the direct inverse method and the modal filtering method. As developed by Okubo et al.,[3] the direct inverse method uses measured frequency response functions to estimate the forces. However, this requires that all points of force application be measurable, which usually is not possible in practical situations. The modal filtering method, conversely, does not have this restriction. Several modal filtering techniques have been developed, e.g., the pseudoinverse method of Desanghere and Snoeys,[4] the reciprocal modal vector method of Zhang et al.,[5] and the modified reciprocal modal vector method of Shelley and Allemang.[6] In these methods, a set of vectors is created (modal filters) that are orthogonal to the substructure's modal vectors. Then, the contribution of each mode is determined by multiplying the forced response by these filters. The modal forces are estimated by dividing the modal responses by the modal frequency response functions corresponding to the individual modes.

There are several disadvantages to the modal filtering method. First, it requires the measurement of at least as many degrees of freedom (DOF) as the number of modal frequencies in the frequency region of interest. This may necessitate the measurement of more points than is desired or required by the CMS representation. Second, the estimated modal forces usually are sensitive to errors in the modal filters. This generally occurs when there is a large difference in modal response magnitudes, such as at a resonant frequency.

Third, modal filtering is sensitive to the location of the measured points, and different locations can give vastly different levels of accuracy. Therefore, the selection of measurement point locations is important.

The new method presented herein bypasses these problems by using superposition of responses instead of force estimation. The procedure considers the internal coupling forces and external applied forces independently and superimposes the responses of each. The response due to the coupling forces is determined using the CMS models. The response due to the applied forces is measured directly. There are several advantages to this approach. First, the new method requires only measurements at the active DOF corresponding to the coupling-forces load case. Active DOF are translations and rotations that are included in the reduced DOF set of the CMS representation. For the coupling-forces load case, they include the coupling DOF and any additional noncoupling DOF selected to be included as active DOF.[1] These are the same DOF required for the calculation of the CMS models, so no additional measurement locations need be included for the calculation of the forced response. Second, the new method theoretically is highly accurate. With error-free response data, the only errors that occur are due to the CMS representation. Third, any number of applied forces can be present, and these can occur at unmeasurable locations. The forced-response calculations are the same regardless of the number and location of the applied forces.

The major contribution of the new method is that it extends the experimentally based method of CMS[1,2] to include forced-response predictions. This allows test-derived models to be coupled to finite element models for forced-response predictions. Finite element models can be analyzed using the test-derived models as dynamic boundary conditions, and operating displacement, acceleration, and stress levels can be predicted.

This paper is organized as follows. The new forced-response method is developed first in Sec. II. The procedure uses experimentally based CMS models. Then, the uncoupled forced response is measured. Next, the forced response due to the coupling forces is calculated, and the results are superimposed and transformed back to the original DOF set. The performance of the new method is demonstrated in Sec. III. A test case is conducted for a simple plate–beam system. The method is first simulated analytically using error-free data, then conducted experimentally using measured data. The experiment illustrates the method's accuracy under practical conditions. Conclusions are drawn in Sec. IV.

II. Forced-Response Method

The new forced-response method uses superposition to divide the loading on a substructure into two load cases. The coupled response then is determined by enforcing the compatibility and equilibrium relations between the various substructures. The applied loading on each substructure is divided into coupling forces between substructures and the remaining externally applied forces, as shown in Fig. 1. The coupled-system forced response is determined by superimposing the responses for the two load cases:

$$\boldsymbol{X} = \hat{\boldsymbol{X}} + \tilde{\boldsymbol{X}} \tag{1}$$

where $\hat{\boldsymbol{X}}$ and $\tilde{\boldsymbol{X}}$ are the responses due to the applied forces and coupling forces, respectively. The response, due to the applied forces,

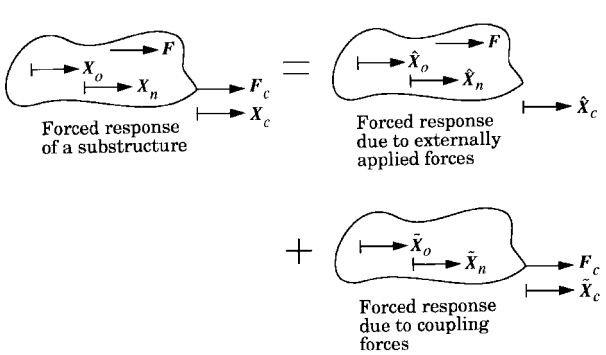

Fig. 1 Superposition of loading.

is measured directly for the uncoupled substructures. The response due to the coupling forces is determined from the CMS models. This method thus involves four major steps, as follows. First, the CMS models are determined from test. Then, the uncoupled responses are measured. Next, the response to the coupling forces is solved. Finally, the total coupled system response is calculated. This is described next.

A. Calculation of the CMS Models

The CMS models are determined using measured frequency response functions shown elsewhere.[1,2] The details are not presented here; however, the resulting CMS matrices are in exactly the same form as in the constraint-modes CMS method of Craig and Bampton.[7] There are four matrices that represent the CMS model of a substructure: transformation, reduced stiffness, mass, and damping matrices. The transformation matrix T_{cb} relates the original DOF to the reduced set

$$\begin{bmatrix} \boldsymbol{X}_o \\ \boldsymbol{X}_a \end{bmatrix} = \begin{bmatrix} \Psi_{oa} & \Upsilon_{os} \\ I_{aa} & 0_{as} \end{bmatrix} \begin{bmatrix} \boldsymbol{X}_a \\ \boldsymbol{X}_s \end{bmatrix} = T_{\text{cb}} \begin{bmatrix} \boldsymbol{X}_a \\ \boldsymbol{X}_s \end{bmatrix} \tag{2}$$

where T_{cb} is a real-valued, non-frequency-dependent matrix. The subscripts a, o, and s indicate the partitioning of the matrices with respect to the active a, omitted o, and modal s DOF. These DOF are selected by considering the location of the coupling forces and the upper frequency limit of interest. Active DOF are selected to include all coupling DOF between substructures, because the CMS models will be used to determine the responses due to the coupling forces. Additionally, enough active DOF must be included so that the resulting CMS representations exhibit no rigid-body modes when all active DOF are constrained (this is a requirement of the Craig–Bampton method). Any selection of omitted DOF is acceptable because these DOF do not affect the calculation of the reduced structural matrices. The modal DOF correspond to the free-boundary modes included in the CMS representation. All free-boundary modes occurring up to 1.0–1.5 times the upper frequency limit of interest should be used. However, rigid-body modes are included as inertia-relief modes.[1]

For the forced-response method, a further partitioning of the active DOF with respect to coupling c and noncoupling n DOF is useful, because all active DOF are not necessarily coupling DOF:

$$\boldsymbol{X}_a = \begin{bmatrix} \boldsymbol{X}_c \\ \boldsymbol{X}_n \end{bmatrix} \tag{3}$$

Equation (2) then becomes

$$\begin{bmatrix} \boldsymbol{X}_o \\ \boldsymbol{X}_c \\ \boldsymbol{X}_n \end{bmatrix} = \begin{bmatrix} \Psi_{oc} & \Psi_{on} & \Upsilon_{os} \\ I_{cc} & 0_{cn} & 0_{cs} \\ 0_{nc} & I_{nn} & 0_{ns} \end{bmatrix} \begin{bmatrix} \boldsymbol{X}_c \\ \boldsymbol{X}_n \\ \boldsymbol{X}_s \end{bmatrix} \tag{4}$$

The reduced stiffness K_{cb} mass M_{cb}, and damping C_{cb} matrices are partitioned likewise and form a dynamic model of the substructure:

$$M_{\text{cb}} \begin{bmatrix} \ddot{\boldsymbol{X}}_c \\ \ddot{\boldsymbol{X}}_n \\ \ddot{\boldsymbol{X}}_s \end{bmatrix} + C_{\text{cb}} \begin{bmatrix} \dot{\boldsymbol{X}}_c \\ \dot{\boldsymbol{X}}_n \\ \dot{\boldsymbol{X}}_s \end{bmatrix} + K_{\text{cb}} \begin{bmatrix} \boldsymbol{X}_c \\ \boldsymbol{X}_n \\ \boldsymbol{X}_s \end{bmatrix} = \begin{bmatrix} \boldsymbol{F}_c \\ \boldsymbol{F}_n \\ \boldsymbol{F}_s \end{bmatrix} \tag{5}$$

This can be transformed into the frequency domain as

$$B_{\text{cb}} \begin{bmatrix} \boldsymbol{X}_c \\ \boldsymbol{X}_n \\ \boldsymbol{X}_s \end{bmatrix} = \begin{bmatrix} B_{cc} & \text{symmetric} & \\ B_{nc} & B_{nn} & \\ B_{sc} & B_{sn} & B_{ss} \end{bmatrix} \begin{bmatrix} \boldsymbol{X}_c \\ \boldsymbol{X}_n \\ \boldsymbol{X}_s \end{bmatrix} = \begin{bmatrix} \boldsymbol{F}_c \\ \boldsymbol{F}_n \\ \boldsymbol{F}_s \end{bmatrix} \tag{6}$$

where $B_{\text{cb}} = K_{\text{cb}} + i\omega C_{\text{cb}} - \omega^2 M_{\text{cb}}$.

B. Forced Response Due to the External Forces

The forced response due to the external forces is determined directly from measurements on the uncoupled substructures. Responses are measured at the active and omitted DOF under the excitation of the applied external forces. Both periodic (deterministic) and stationary random (nondeterministic) forces may occur. For periodic forces, standard signal processing and response averaging can be used, provided a reliable reference trigger can be identified. Stationary random excitations also can be handled using the method of

virtual sources developed by Warwick and Gilheany.[8] The method of solution is the same, so only periodic forces are considered herein. The measured forced response due to the external forces on a substructure then is partitioned as

$$\hat{\boldsymbol{X}} = \begin{bmatrix} \hat{\boldsymbol{X}}_o \\ \hat{\boldsymbol{X}}_c \\ \hat{\boldsymbol{X}}_n \end{bmatrix} \tag{7}$$

C. Forced Response Due to the Coupling Forces

For forces applied at the coupling DOF, $\boldsymbol{F}_n$ and $\boldsymbol{F}_s$ in Eq. (6) are zero vectors. This allows the forced response due to the coupling forces to be determined using the CMS models. The forced response due to the coupling forces can be solved by enforcing the compatibility and equilibrium relations between substructures. Compatibility between substructures requires that the coupled responses at the coupling DOF be equal for all connected substructures:

$$\boldsymbol{X}_c^{(1)} = \boldsymbol{X}_c^{(2)} = \ldots = \boldsymbol{X}_c^{(N)} = \boldsymbol{X}_c \tag{8}$$

where the superscript corresponds to a particular substructure. From Eq. (1), $\boldsymbol{X}_c = \hat{\boldsymbol{X}}_c + \tilde{\boldsymbol{X}}_c$. Solving for $\tilde{\boldsymbol{X}}_c$ in terms of $\boldsymbol{X}_c$ and $\hat{\boldsymbol{X}}_c$, and substituting into Eq. (6) with $\boldsymbol{F}_n = \boldsymbol{0}$ and $\boldsymbol{F}_s = \boldsymbol{0}$, gives

$$\begin{bmatrix} B_{cc} & \text{symmetric} & \\ B_{nc} & B_{nn} & \\ B_{sc} & B_{sn} & B_{ss} \end{bmatrix} \begin{bmatrix} \boldsymbol{X}_c \\ \tilde{\boldsymbol{X}}_n \\ \tilde{\boldsymbol{X}}_s \end{bmatrix} = \begin{bmatrix} \boldsymbol{F}_c + B_{cc}\hat{\boldsymbol{X}}_c \\ B_{nc}\hat{\boldsymbol{X}}_c \\ B_{sc}\hat{\boldsymbol{X}}_c \end{bmatrix} \tag{9}$$

Then, the coupled substructure system matrices can be assembled. The general form of the assembled system is

$$[\text{Assembled System Matrix}] \begin{bmatrix} \tilde{\boldsymbol{X}}_n^{(1)} \\ \tilde{\boldsymbol{X}}_n^{(2)} \\ \cdots \\ \tilde{\boldsymbol{X}}_n^{(N)} \\ \boldsymbol{X}_c \\ \tilde{\boldsymbol{X}}_s^{(1)} \\ \tilde{\boldsymbol{X}}_s^{(2)} \\ \cdots \\ \tilde{\boldsymbol{X}}_s^{(N)} \end{bmatrix} = \begin{bmatrix} B_{nc}^{(1)}\hat{\boldsymbol{X}}_c^{(1)} \\ B_{nc}^{(2)}\hat{\boldsymbol{X}}_c^{(2)} \\ \cdots \\ B_{nc}^{(N)}\hat{\boldsymbol{X}}_c^{(N)} \\ \sum_{0}^{N} \boldsymbol{F}_c^{(j)} + \sum_{}^{N} B_{cc}^{(j)}\hat{\boldsymbol{X}}_c^{(j)} \\ B_{sc}^{(1)}\hat{\boldsymbol{X}}_c^{(1)} \\ B_{sc}^{(2)}\hat{\boldsymbol{X}}_c^{(2)} \\ \cdots \\ B_{sc}^{(N)}\hat{\boldsymbol{X}}_c^{(N)} \end{bmatrix} = \bar{\boldsymbol{F}} \tag{10}$$

As indicated, the assembly process automatically groups the coupling forces together. These cancel out, so that equilibrium between substructures is preserved:

$$\sum_{}^{N} \boldsymbol{F}_c^{(j)} = \boldsymbol{0} \tag{11}$$

Equation (10) represents the forced response of the coupled system due to a known external force vector $\bar{\boldsymbol{F}}$. Standard methods can be used to solve for the response. Then, the responses due to the coupling forces are determined for each substructure as

$$\begin{bmatrix} \tilde{\boldsymbol{X}}_o \\ \tilde{\boldsymbol{X}}_c \\ \tilde{\boldsymbol{X}}_n \end{bmatrix} = \begin{bmatrix} \Psi_{oc} & \Psi_{on} & \Upsilon_{os} \\ I_{cc} & 0_{cn} & 0_{cs} \\ 0_{nc} & I_{nn} & 0_{ns} \end{bmatrix} \begin{bmatrix} \boldsymbol{X}_c \\ \tilde{\boldsymbol{X}}_n \\ \tilde{\boldsymbol{X}}_s \end{bmatrix} + \begin{bmatrix} -\Psi_{oc} \\ -I_{cc} \\ 0_{nc} \end{bmatrix} \hat{\boldsymbol{X}}_c \tag{12}$$

D. Superposition of Forced Responses

The forced response of the coupled system is determined by superimposing the responses for the two load cases:

$$\begin{bmatrix} \boldsymbol{X}_o \\ \boldsymbol{X}_c \\ \boldsymbol{X}_n \end{bmatrix} = \begin{bmatrix} \hat{\boldsymbol{X}}_o \\ \hat{\boldsymbol{X}}_c \\ \hat{\boldsymbol{X}}_n \end{bmatrix} + \begin{bmatrix} \tilde{\boldsymbol{X}}_o \\ \tilde{\boldsymbol{X}}_c \\ \tilde{\boldsymbol{X}}_n \end{bmatrix} \tag{13}$$

Substituting Eq. (12) into Eq. (13) gives the desired coupled-system forced response:

$$\begin{bmatrix} \boldsymbol{X}_o \\ \boldsymbol{X}_c \\ \boldsymbol{X}_n \end{bmatrix} = \begin{bmatrix} I_{oo} & -\Psi_{oc} & 0_{on} \\ 0_{co} & 0_{cc} & 0_{cn} \\ 0_{no} & 0_{nc} & I_{nn} \end{bmatrix} \begin{bmatrix} \hat{\boldsymbol{X}}_o \\ \hat{\boldsymbol{X}}_c \\ \hat{\boldsymbol{X}}_n \end{bmatrix} + \begin{bmatrix} \Psi_{oc} & \Psi_{on} & \Upsilon_{os} \\ I_{cc} & 0_{cn} & 0_{cs} \\ 0_{nc} & I_{nn} & 0_{ns} \end{bmatrix} \begin{bmatrix} \boldsymbol{X}_c \\ \tilde{\boldsymbol{X}}_n \\ \tilde{\boldsymbol{X}}_s \end{bmatrix} \tag{14}$$

III. Test Case: Forced Response of a Plate–Beam System

The new method was validated using the coupled plate–beam system shown in Fig. 2. The plate is externally excited by a single force located at point 9. The force features an input spectrum of unity magnitude and zero phase from 0 to 1000 Hz. Coupling between the beam and the plate occurs between points 2 and 6 in the form of a threaded steel spike. This roughly approximates a pin joint that couples the system in the translational DOF only. Therefore, only translational DOF need to be included in the CMS models, and no rotational DOF need to be measured.

Two validation tests were conducted. The first test was an analytical simulation of the method using error-free response data. This demonstrates the effectiveness of the method under idealized conditions. The second test was an experimental implementation of the method using measured data. This demonstrates the performance of method under practical conditions. Because the accuracy of the forced-response predictions depends on the accuracy of the calculated modal properties of the coupled system, the natural frequencies and modal assurance criterion (MAC) values are determined first.[9] Then, the forced responses at points 1, 6, and 8 are compared. These points are selected because they represent an active noncoupling DOF, active coupling DOF, and an omitted DOF, respectively.

A. Analytical Results

The analytical simulation of the method was conducted using finite element analysis (FEA). The frequency region from 0 to 1000 Hz was considered as the frequency region of interest. Steel material properties were used for both the plate and the beam. The assumed material properties are as follows: modulus of elasticity $E = 1.95 \times 10^{11}$ Pa, mass density $\rho = 7700\ \text{kg/m}^3$, Poisson's ratio $\upsilon = 0.28$, and structural damping coefficient $\alpha = 0.002$.

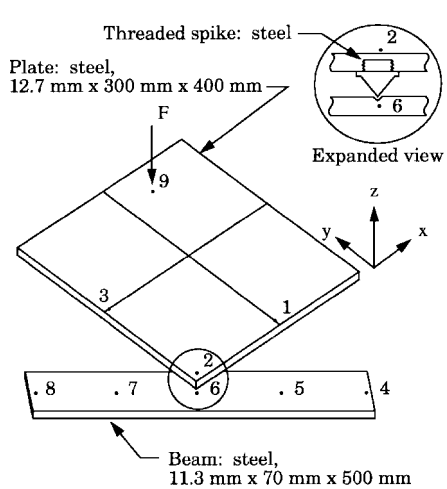

Fig. 2 Test case: forced response of a plate–beam system; free-free boundary conditions.

The plate was modeled using a rectangular grid corresponding to $x = 0.0, 0.1, 0.15, 0.2$, and 0.3 m and $y = 0.0, 0.075, 0.2, 0.325$, and 0.4 m, as defined by the coordinate system shown in Fig. 2. The intersection of these lines determines the grid points in the finite element model. Only transverse deflection is considered. Therefore, each grid point has one translational and two rotational DOF. This results in a model with 16 rectangular plate elements and 75 DOF. The local stiffness matrices of the rectangular plate elements were determined directly from the tabulated results of Zienkiewicz and Cheung,[10] for nonconforming shape functions. The local mass matrices were determined from the tabulated results of Dawe,[11] for the same nonconforming shape functions.

The beam was modeled using grid points centered across the width and evenly distributed lengthwise every 25 mm. Each grid point has an associated translational and rotational DOF; thus, a finite element model with 20 linear beam elements and 42 DOF is obtained. Bernoulli–Euler beam theory was employed with transverse deflection in each beam segment modeled using Hermite cubic interpolation functions, and consistent mass matrices were used.[12]

The CMS matrices were calculated using the residual flexibility method, and then were transformed to Craig–Bampton form.[1] The translational DOF at points 1–3 on the plate were selected as active, with the remaining DOF selected as omitted. The translational DOF at points 4 and 6 on the beam were selected as active, with the remaining DOF selected as omitted. All free-boundary modes that occur in the frequency region of interest (0–1000 Hz) were included. For the plate, three rigid-body and five flexural modes were included. For the beam, two rigid-body and two flexural modes were included.

The coupling stiffness was calculated from the theoretical stiffness of a frustrum of a cone:

$$k_c = \frac{\pi d_o^2 E}{4L^2[1/(L - S) - (1/L)]} \tag{15}$$

where the base diameter ($d_o = 5$ mm), the modulus of elasticity for steel ($E = 1.95 \times 10^{11}$ Pa), the length of the cone to the theoretical tip ($L = 8$ mm), and the length of the cone to the truncated surface ($S = 7.5$ mm) are estimated from the threaded spike and pilot mark in the beam. The resulting coupling stiffness is $k_c = 3.2 \times 10^7$ N/m.

The plate's uncoupled forced response was determined using the unreduced FEA matrices. Similarly, the exact coupled forced response was determined using the FEA matrices and coupling stiffness, with the applied load as specified. The coupled CMS modal properties and MAC values were calculated and are compared to the exact ones in Table 1. Because error-free data are used, the coupled-system predictions using the CMS models are very accurate. The forced response was determined using the new method. The responses at points 1, 6, and 8 are shown in Figs. 3–5. The results are very accurate. The only errors that occur are near the end of the frequency region of interest, where the residual effects of the omitted modes are not fully accounted for in the CMS representations.

B. Experimental Results

The method was conducted experimentally using the test setup shown in Fig. 6. The plate and beam were each tested individually, then coupled together. A threaded steel spike was used to couple the plate and beam. The plate was tapped to accept the spike and a pilot mark was indented into the beam using a center punch. The spike rested in this pilot mark and was held in contact with the beam by the weight of the plate. This roughly approximated a pin joint with zero rotational stiffness and large translational stiffness. The translational stiffness was approximated using the theoretical stiffness of a frustrum of a cone, as shown in Sec. III.A.

Table 1 Analytical modal parameter comparison for the coupled system

	Frequency, Hz		Damping factor, %		MAC
Mode no.	FEA	CMS	FEA	CMS	value
1	166	166	0.10	0.10	1.00
2	284	284	0.10	0.10	1.00
3	382	382	0.10	0.10	1.00
4	559	559	0.10	0.10	1.00
5	645	645	0.10	0.10	1.00
6	748	748	0.10	0.10	1.00
7	888	891	0.10	0.10	1.00

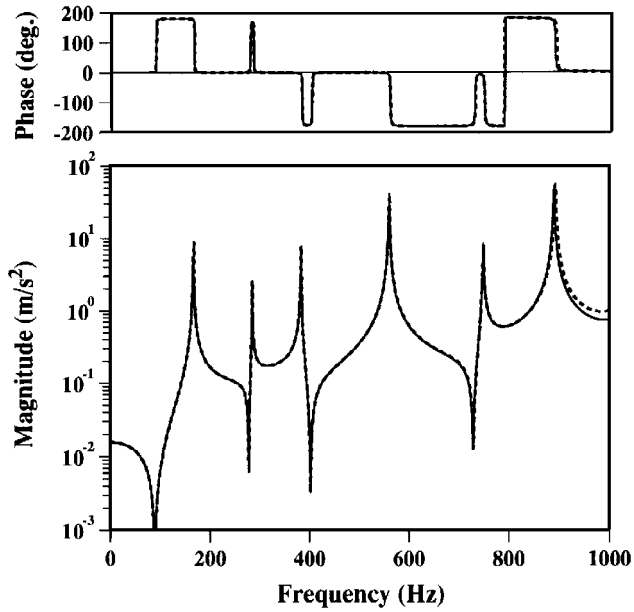

Fig. 3 Analytical FEA (——) and CMS (----) forced response at point 1.

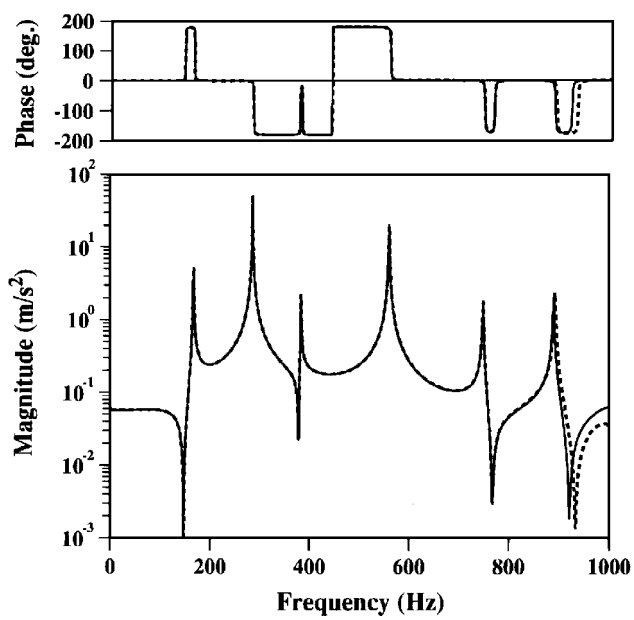

Fig. 4 Analytical FEA (——) and CMS (----) forced response at point 6.

Impact excitation was used to simulate the force at point 9. Each impact was scaled to unity magnitude and zero phase. To eliminate the need for windowing the response time records, system damping was increased by applying viscoelastic damping material (E-A-R Speciality Composites Div., Cabot Safety Corp., 7911 Zionsville Rd., Indianapolis, IN 56268) to one side of both the plate and the beam. This caused the time signals to decay to approximately zero at the end of the time records. Thus, leakage errors in the calculated response spectrums were reduced. This damping augmentation was carried out only to simplify the test case. Actual implementations of the method would use existing windowing and signal processing methods to measure the steady-state forced response of the structure under the operating excitations. However, the implementation of the method was unchanged by increasing the damping.

The data required to conduct the experimental implementation were determined using six tests, as shown in Table 2. Tests 1–3, 5, and 6 were used to calculate the frequency response functions required for the CMS models. Test 4 was used for the uncoupled forced-response measurement.

The experimentally based CMS models were determined using the method of Morgan et al.[1,2] The procedure involves five major steps. First, the frequency response functions are experimentally measured. Then, both global and local estimates of the modal parameters corresponding to the included modes are determined. Next, the approximate residual functions are optimized and the matrices corresponding to the computational modes are determined. The residual flexibility matrices then are assembled from the test-derived data. Finally, the residual flexibility matrices are transformed to Craig–Bampton form, using the two-stage transformation.

Table 2 Description of experimental tests

Test no.	Test configuration	Driving point	Type of test
1	Uncoupled plate	1, z	Modal test
2	Uncoupled plate	2, z	Modal test
3	Uncoupled plate	3, z	Modal test
4	Uncoupled plate	9, $\_z$	Forced-response test
5	Uncoupled beam	4, z	Modal test
6	Uncoupled beam	6, z	Modal test

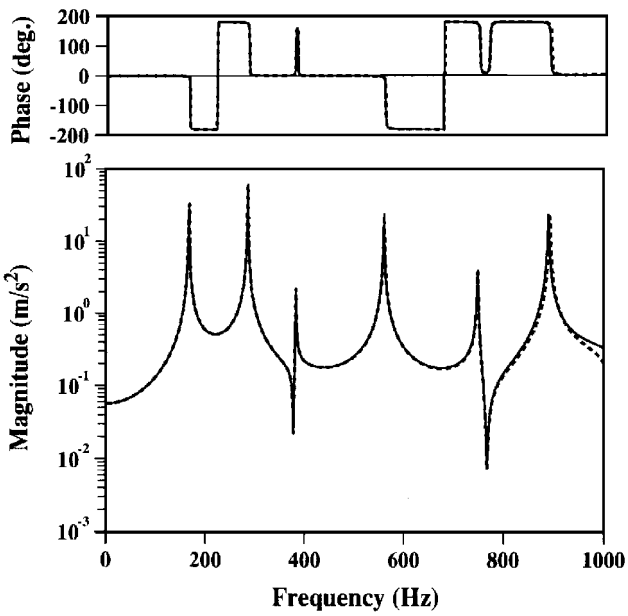

Fig. 5 Analytical FEA (——) and CMS (- - - -) forced response at point 8.

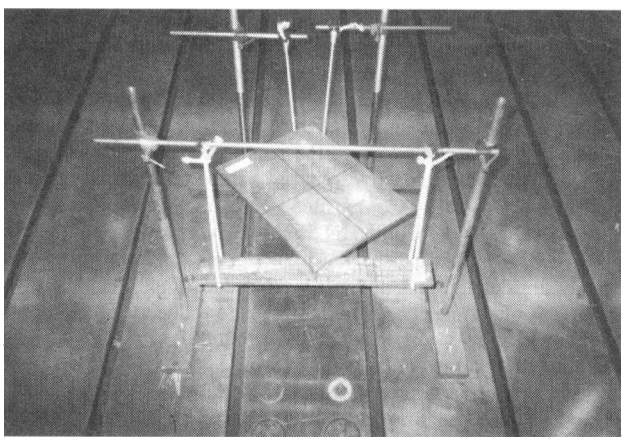

Fig. 6 Experimental test setup.

Frequency response functions were measured with free-boundary conditions applied to the active DOF, as required for the experimentally based method. The same selection of active DOF was used as for the analytical simulation. Points 5, 7, and 8 were the only measured omitted DOF. Impact excitation was used. All vibrational modes that occurred in the frequency region of interest (0–1000 Hz) were included in the CMS representations. As was the case for the analytical simulation, three rigid-body and five flexural modes were included for the plate, and two rigid-body and two flexural modes were included for the beam. The rigid-body modes were calculated from the FEA models and were included in the representation with zero damping.

Exact residual functions were determined by subtracting the curve-fit modes from the measured frequency response functions. These residual functions were characterized as either type I or type II, based on the absence or presence of an antiresonance between 0 Hz and the frequency of the first omitted high-frequency mode, respectively. Approximate residual functions were determined to represent the effects of the omitted modes using the optimization procedure presented previously.[1,2] Then, the matrices corresponding to the computational modes were determined, and the residual flexibility matrices were assembled and transformed to the Craig–Bampton type.

The individual plate and beam CMS matrices were assembled with the coupling stiffness, and the resulting eigenvalue problem was solved for the modal properties of the coupled system. A modal test then was conducted on the coupled system and the measured natural frequencies and modal vectors were determined. The comparison between the predicted and measured results is shown in Table 3. Frequency correlation is good, with the maximum error being $\_7.4\%$. Damping correlation is good, except for modes 1 and 4, which have much higher measured values. It is surmised that this discrepancy was caused by the uncertainties in the contact at the plate-beam interface. Also, the impact excitation, rather than a resonant excitation, presumably contributed to the errors in the damping factors. The MAC values indicate that the modal vectors also correlate well.

The forced response of the coupled system was predicted using the new method. In addition, the forced response was measured so that the predicted results could be compared to actual measured results. The resulting responses at points 1, 6, and 8 are shown in Figs. 7–9. The results are reasonably accurate. The responses at the other DOF are of similar accuracy. This shows that accurate forced-response predictions for systems of coupled substructures

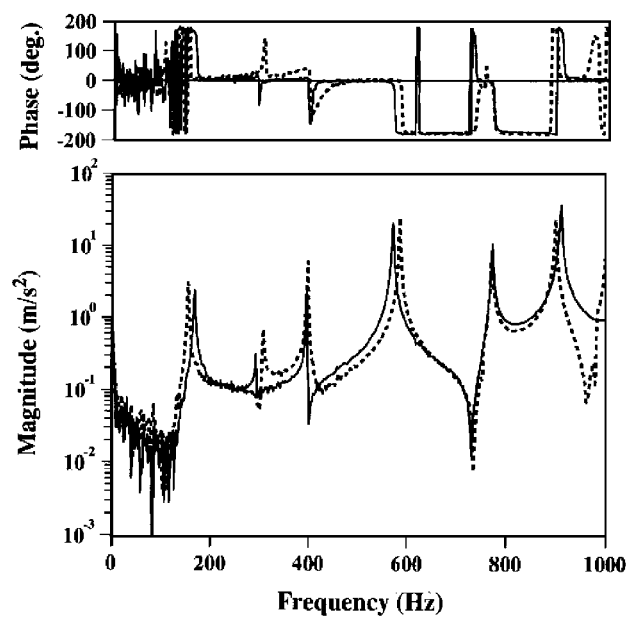

Fig. 7 Experimental measured (——) and CMS (- - - -) forced response at point 1.

Table 3 Experimental modal parameter comparison for the coupled system

Mode no.	Frequency, Hz		Damping factor, %		MAC value
	Meas.	CMS	Meas.	CMS	
1	165	153	0.86	0.10	0.98
2	291	305	0.22	0.19	0.97
3	394	396	0.10	0.11	0.99
4	572	582	0.57	0.11	0.98
5	640	640	0.17	0.12	0.97
6	770	769	0.18	0.15	1.00
7	907	897	0.16	0.12	0.92

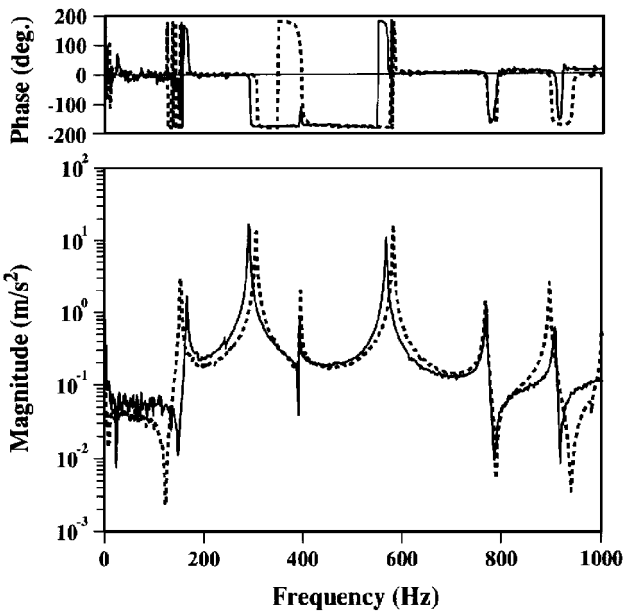

Fig. 8 Experimental measured (——) and CMS (- - - -) forced response at point 6.

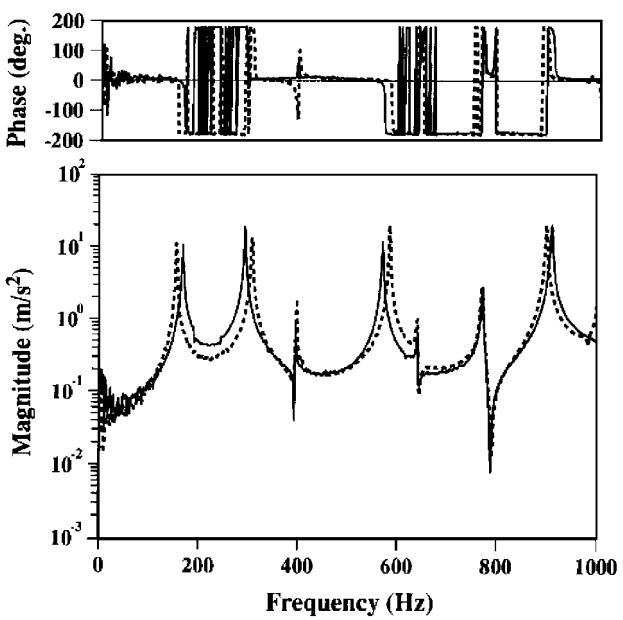

Fig. 9 Experimental measured (——) and CMS (- - - -) forced response at point 8.

can be determined using test-derived CMS matrices and uncoupled forced-response data.

IV. Conclusion

A method has been developed that allows the forced response of a system of coupled substructures to be determined from uncoupled response data. The method uses experimentally based CMS models and measured response data. A simple test case of a coupled plate–beam system was used to evaluate the method. The method was shown to be very accurate when error-free data were used. Reasonable accuracy was achieved in the experimental implementation of the method. It is expected that the main application of the new method will be for integrating test-derived models and FEA models for forced-response predictions. Test-derived models are generated for components that exist in hardware, and FEA models are generated for the remaining components. The new method allows the coupled-system forced response to be predicted. This allows new designs to be evaluated and optimized based on coupled-system forced-response requirements such as displacement, acceleration, and stress criteria, without having to generate FEA models for the entire system. For more complicated systems, coupling will occur at rotational DOF. Therefore, both rotational accelerometers and moment excitation devices will need to be developed. Additionally, more detailed representations of the coupling interfaces, including damping effects, should be investigated.

Acknowledgment

The first author gratefully acknowledges the support by General Motors Corporation under a research fellowship.

References

[1] Morgan, J. A., Pierre, C., and Hulbert, G. M., "Calculation of Component Mode Synthesis Matrices from Measured Frequency Response Functions Part I: Theory," *Journal of Vibration and Acoustics* (to be published).

[2] Morgan, J. A., Pierre, C., and Hulbert, G. M., "Calculation of Component Mode Synthesis Matrices from Measured Frequency Response Functions Part II: Application," *Journal of Vibration and Acoustics* (to be published).

[3] Okubo, N., Tanabe, S., and Tatsuno, T., "Identification of Forces Generated by a Machine Under Operating Condition," *Proceedings of the Third International Modal Analysis Conference*, Union College, Schenectady, NY, 1985, pp. 920–927.

[4] Desanghere, G., and Snoeys, R., "Indirect Identification of Excitation Forces by Modal Coordinate Transformation," *Proceedings of the Third International Modal Analysis Conference*, Union College, Schenectady, NY, 1985, pp. 685–690.

[5] Zhang, Q., Shih, C. Y., and Allemang, R. J., "Orthogonality Criterion for Experimental Modal Vectors," American Society of Mechanical Engineers, Publication DE, Vol. 18-4, New York, 1989, pp. 251–258.

[6] Shelley, S. J., and Allemang, R. J., "Calculation of Discrete Modal Filters Using the Modified Reciprocal Modal Vector Method," *Proceedings of the Tenth International Modal Analysis Conference*, Union College, Schenectady, NY, 1992, pp. 37–45.

[7] Craig, R. R., Jr., and Bampton, M. C. C., "Coupling of Substructures for Dynamic Analyses," *AIAA Journal*, Vol. 6, No. 7, 1968, pp. 1313–1319.

[8] Warwick, D. C., and Gilheany, J. J., "Dynamic Force Estimation via Modal Decomposition of Operational Response Measurements in a Multi-Source Environment," *Proceedings of the Eleventh International Modal Analysis Conference*, Union College, Schenectady, NY, 1993, pp. 278–285.

[9] Allemang, R. J., and Brown, D. L., "A Correlation Coefficient for Modal Vector Analysis," *Proceedings of the First International Modal Analysis Conference*, Union College, Schenectady, NY, 1982, pp. 110–116.

[10] Zienkiewicz, O. C., and Cheung, Y. K., *The Finite Element Method in Structural and Continuum Mechanics*, McGraw–Hill, London, 1967, pp. 95–97.

[11] Dawe, D. J., "A Finite Element Approach to Plate Vibration Problems," *Journal of Mechanical Engineering Science*, Vol. 7, No. 1, 1965, pp. 28–32.

[12] Strang, W. G., and Fix, G. J., *An Analysis of the Finite Element Method*, Prentice–Hall, Englewood Cliffs, NJ, 1973, p. 58.